UCLA
COMPUTATIONAL AND APPLIED MATHEMATICS

Diffusion-Generated Motion by Mean Curvature for Filaments

Steven J. Ruuth

Barry Merriman

Jack Xin

Stanley Osher

November 1998

(Revised September 2001)

CAM Report 98-47

Diffusion-Generated Motion by Mean Curvature for Filaments

Steven J. Ruuth[1]

Barry Merriman[2]

Jack Xin[3]

Stanley Osher[4]

Abbreviated title: Diffusion Generated Motion for Filaments.

Abstract

Diffusion-generated motion by mean curvature is a simple algorithm for producing motion by mean curvature of a surface, in which the motion is generated by alternately diffusing and renormalizing a characteristic function. In this paper, we generalize diffusion-generated motion to a procedure that can be applied to the curvature motion of filaments, i.e. curves in R^3, that may initially consist of a complex configuration of links. The method consists of applying diffusion to a complex valued function whose values wind around the filament, followed by normalization. We motivate this approach by considering the essential features of the complex Ginzburg-Landau equation, which is a reaction-diffusion PDE that describes the formation and propagation of filamentary structures. The new algorithm naturally captures topological merging and breaking of filaments without fattening curves. We justify the new algorithm with asymptotic analysis and numerical experiments.

1 Introduction

Diffusion-generated motion by mean curvature is a particularly simple and robust algorithm for producing motion by mean curvature of a surface [15, 16]. The major goal underlying this work is to generalize this algorithm from surfaces (dimension $d - 1$ inside R^d) to the motion by curvature of a curve—or "filament"—in three dimensions.

The motion of filaments is of particular interest because many physical and mathematical systems exhibit the formation and propagation of filamentary structures. Notable examples include magnetic flux tubes trapped in superconductors, vortex filaments in inviscid fluids, the centers of scroll waves in excitable media, biological polymers such as protein and DNA, and skeleton curves extracted from processing 3-D images in computer vision.

Asymptotic models for these processes often yield equations of motion for a curve moving with a velocity that is a function of its local geometry, i.e. a function of the local normal and binormal direction, curvature, torsion, and higher space and time derivatives of these quantities. For example, studies of models for superconductors and excitable media predict that their vortex filaments evolve asymptotically with a speed proportional to curvature [5, 26].

Given such models, it becomes important to consider algorithms which can realize geometric filament motions in simple, efficient and accurate ways, and which are amenable to mathematical analysis. Designing suitable algorithms is complicated by the fact that in many problems the filaments can merge or break up. It is particularly challenging to find algorithms that retain their simplicity, yet are robust enough to capture these topological transitions.

For surfaces (or, generally, codimension one objects) the level set method of Osher and Sethian [18] was introduced to compute (and define) arbitrary curvature-dependent surface motions, including topological changes. This provides a PDE based method for motion by mean curvature, including the pinch-offs which can occur in three dimensions. Standard numerical PDE methods apply to accurately discretize the equations of motion. However, the original level set method does not directly apply to objects of higher codimension, such as filaments. The level set method was ultimately extended to arbitrary codimension [1, 3]. In the earlier approach [1], the object is represented by its squared distance function, or any other similar smooth function. Unfortunately, the representation is not robust: A perturbation

of the level set function φ can inadvertently break up the filament since its representation is given by $\{\vec{x} : \varphi(\vec{x}) < \epsilon\}$ for a small, positive ϵ and $\varphi \geq 0$. Also, the method has the undesirable property that filaments tend to develop interiors whenever mergers occur. See [2] for a detailed discussion on this "fattening phenomenon." Alternatively, the filament can be (robustly) represented as the intersection of two level set functions. See [3] for details on this recent method.

The curvature motion of filaments (or the mean curvature motion of surfaces) may also be approximated using reaction-diffusion models such as the complex Ginzburg-Landau equation. Briefly, these methods have the important advantage that they automatically capture the curvature motion of filaments including topological change without fattening curves. When used in computation, however, the spatial discretization must resolve a thin reaction zone in order to accurately compute the motion. Since the width of the front is $O(\epsilon)$, the only remedy is to use a mesh spacing which is much less than ϵ, which can be impractical numerically [16].

In the case of surface motion, a simplified algorithm based on an idealization of reaction-diffusion was presented in [15, 16]. This algorithm essentially consists of moving a set boundary by alternately "diffusing" the set—i.e. applying the linear diffusion evolution equation to the set's characteristic function for a short time—and then recovering a new set via a "sharpening" step in which values of the diffused characteristic function are re-normalized to 0 or 1, whichever is closer. This "diffusion-generated motion by mean curvature" algorithm automatically captures topological change and has a direct extension to a variety of interesting anisotropic motions [9, 23, 10] as well as the motion of triple point junctions [15, 14, 16, 21]. It naturally provides the fine grid limit of an interesting variety of cellular automata models [24]. See also [7, 6] for some related biological models. Diffusion-generated motion has the advantage that it can be discretized efficiently and accurately since the highest frequency modes never need to be approximated (they are eliminated by diffusion and do not interact with other modes during the main diffusion step). Moreover, adaptive grid refinement is straightforward since it is carried out as a quadrature using unequally spaced fast Fourier transforms [22]. Unfortunately, the original method does not apply to objects with higher codimension, such as filaments.

In this present work, we generalize the original diffusion generated motion algorithm to filaments which are fibered links, via a natural idealization

4

of the complex Ginzburg-Landau model. This diffusion-generated filament motion naturally computes the (vector) mean curvature motion, including topological changes without curve fattening. The method has the potential for a variety of extensions. Similar to the usual diffusion-generated motion algorithm, the method may be discretized to give improved computational efficiency over reaction-diffusion models. While simple, our proposed algorithm is still not practical for generating highly accurate solutions to curvature motion since the local truncation error is $O(1/|\log(\Delta t)|)$. (See Section 3.) To achieve higher accuracy, the level set method for filaments may be used. See [3] for details.

The outline of the paper is as follows. Section 2 begins by reviewing the complex Ginzburg-Landau equation. Using this phase field model as an inspiration and motivation, a diffusion-generated algorithm for the curvature-dependent motion of filaments is derived. In Section 3, we give an asymptotic justification that diffusion-generated filament motion gives motion by curvature in the normal direction. Section 4 reports on a variety of experiments validating our algorithm. Finally, in Section 5 we discuss other possible variations on this approach.

2   Diffusion-Generated Motion of Filaments

In this section, we review the complex Ginzburg-Landau model for evolving filaments with a normal velocity equal to the (vector) curvature. Then, we idealize this reaction-diffusion model to obtain a diffusion-generated algorithm for the curvature-dependent motion of filaments in three dimensions. Later sections will justify our proposed method with asymptotics and numerical experiments, and also extend it to arbitrary dimensions and codimensions.

2.1   The Complex Ginzburg-Landau Equation

The complex Ginzburg-Landau equation is:

$$u_t = \Delta u - \frac{1}{\epsilon^2} u(|u|^2 - 1), \tag{1}$$

where $u(x, t)$ is a complex scalar and $0 < \epsilon \ll 1$ is a basic model for understanding the motion of phase defects (singularities). For $\vec{x} \in R^3$ the defects

are generically supported on the one dimensional curve (filament) where $|u^\epsilon|$ vanishes. Equation (1) is the magnetic field-free case of the time dependent Ginzburg-Landau system, which models the mixed states in type-II superconductors where magnetic flux carrying normal filaments are embedded in a superconducting matrix, [5]. The complex scalar u^ϵ is an order parameter, representing normal phase if $|u^\epsilon|$ is close to zero and super phase if close to one, and $\epsilon \ll 1$ is the effective diameter of the magnetic flux core. Equation (1) is also a generic amplitude equation describing instabilities near bifurcation points in dissipative systems, known as the Landau-Stuart equation, [12].

Asymptotic analysis can be used to extract the $\epsilon \to 0$ limiting behavior of solutions. For initial data $u(x, 0)$ vanishing on a filament Γ_0 and having winding number one around it, formal asymptotic derivation [19] shows that solution evolves to leading order as a complex scalar vanishing along the filament Γ_t which is generated from Γ_0 as motion by curvature along the normal. If the filaments are nearly parallel, rigorous results are established in [13] on their dynamics on the $O(\log \frac{1}{\epsilon})$ time scale.

Numerically, small ϵ introduces small length and time scales into the dynamics. Consequently, an accurate direct simulation of (1) has to resolve the core size and reaction rate, an expensive task in three dimensions. However, it turns out we can capture the desired limiting filament dynamics with a complex diffusion-generated motion algorithm obtained by idealizing the effect of the strong reaction in (1).

2.2 Complex Diffusion-Generated Motion

Similar to the case of diffusion-generated motion, a formal splitting method can be applied to the complex Ginzburg-Landau equation to obtain an algorithm for motion by mean curvature of filaments. In the reaction step, an initial complex-valued $\chi(\vec{x}, t_0)$ is driven towards one of its stable equilibrium values $e^{i\theta}$ by the reaction kinetics,

$$\bar{\chi}_t = -\frac{1}{\epsilon^2}\bar{\chi}(|\bar{\chi}|^2 - 1)$$
$$\bar{\chi}(\vec{x}, 0) = \chi(\vec{x}, t_0)$$

for a time Δt to obtain an intermediate result $\bar{\chi}(\vec{x}, \Delta t)$. This result is subsequently diffused for a time Δt,

$$\chi_t = \nabla^2 \chi$$
$$\chi(\vec{x}, t) = \bar{\chi}(\vec{x}, \Delta t)$$

to obtain the desired update $\chi(\vec{x}, t_0 + \Delta t)$. By replacing the reaction step by its formal limit as $\epsilon \to 0$, it becomes the simple normalization to a unit complex number

$$\bar{\chi} = \frac{\chi}{|\chi|}$$

and we obtain the following method for (hopefully) evolving filaments with a normal velocity equal to curvature:

ALGORITHM **CDGM**
GIVEN: An initial filament.

BEGIN
    (1) "Initialize": Set χ so that its "center of winding" coincides with the filament. I.e. set χ so that its winding number is nonzero around any closed curve that winds around the filament. See next section.
    (2) Repeat for all steps:
        (a) "Normalize": $\bar{\chi} = \frac{\chi}{|\chi|}$
        (b) "Diffuse": Starting from $\bar{\chi}$, evolve χ for a time Δt according to $\chi_t = \nabla^2 \chi$.
END

The location of the interface is given by the zero contour of χ (or, equivalently, its center of winding, though this is more difficult to locate in practice).

As we shall see in the analysis of Section 3, this simple splitting method captures the leading order behavior of the complex Ginzburg-Landau equation: I.e., it produces a normal velocity equal to the curvature of the filament without ever directly computing curvature. Topological mergers are also captured with no special algorithmic procedures. In particular, filaments do not develop interiors (unlike level set methods for filament motion — see [2]) and a good agreement with optimal curve shortening is observed.

We now complete our description of the algorithm with a discussion on the initialization of χ.

2.3 Initialization of χ

To apply the ALGORITHM **CDGM**, an initial value of χ is required.

If the filament is already defined implicitly as the zero of a function u arising from a complex Ginzburg-Landau equation, then we simply set $\chi = u$ to initialize. But, in general, we need to construct a $\chi : R^3 \rightarrow C$ which implicitly captures the position of the filament. We use the same representation as in the complex Ginzburg-Landau equation. Specifically, we construct a complex-valued χ so that the winding number of $\chi(\vec{x})$ (with respect to zero in the complex plane) is nonzero when $\vec{x}$ moves around any closed loop that encircles the filament. Along other loops, however, the winding number must be zero to avoid creating spurious filaments.

It is natural to ask whether an interesting variety of curves can be represented in this manner. The answer to this question arises in the study of Ginzburg-Landau flow [20]. Specifically, a large number of initial conditions are possible since this filament representation corresponds to curves that are fibered links [20]. See [17] for a systematic construction of χ for a given fibered link.

In this paper, we define planes and reference axis through each point on the filament, so that the planes fill out R^3 (see Fig. 1a). The initialization on a particular plane is then given by $\chi(\vec{x}) = \exp(i\theta(\vec{x}))$ where $\theta(\vec{x})$ the angle function in that plane, measured relative to the reference axis in the plane. As shown in Fig. 1b, this type of initialization is particularly straightforward whenever the filament can be represented as a function of z in some coordinate system. Looping structures such as rings and linked rings are also easily initialized in this manner. See Section 4. Alternatively, whenever two surfaces can be found whose intersection gives the desired filament, a simple shape-based initialization can be used. See [25] for details and examples for this alternative.

We now direct our attention to the convergence analysis of our proposed algorithm.

3 Analysis of Diffusion-Generated Motion

In this section, we present formal analyses which show that the diffusion generated motion algorithm for filaments does produce a time discrete approx-
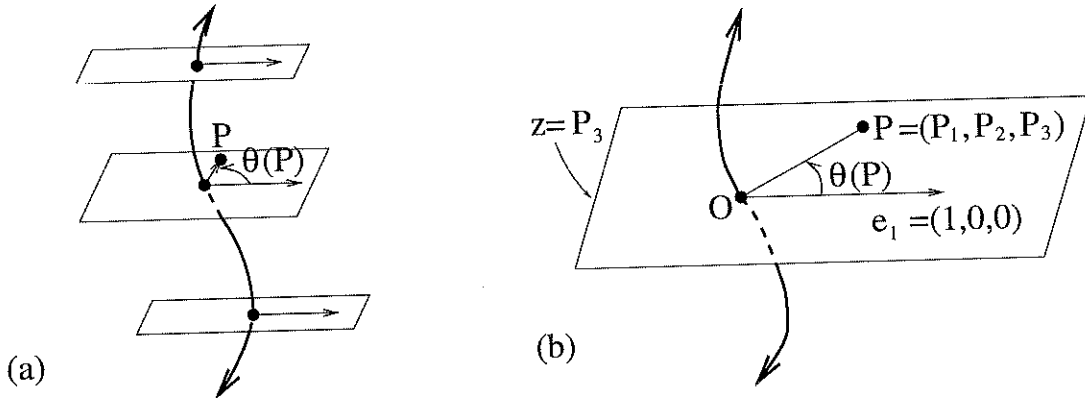
Figure 1: (a) In our examples, a plane and a reference axis are defined for each point on the filament. The initialization for a particular plane is then given by $\chi(\mathbf{P}) = \exp(i\theta(\mathbf{P}))$ where $\theta(\mathbf{P})$ is an angle function that winds around the filament. (b) Whenever the curve can be represented as a function of z in some coordinate system, this initialization step is particularly straightforward. For each grid point $\mathbf{P} = (P_1, P_2, P_3)$ we restrict ourselves to the plane $z = P_3$ and set $\mathbf{O}$ equal to the intersection of the plane with the curve. A consistent initialization is then obtained by setting $\chi(\mathbf{P}) = \exp(i\theta(\mathbf{P}))$ where $\theta(\mathbf{P})$ is the angle between $\mathbf{OP}$ and the fixed vector $\mathbf{e_1} = (1, 0, 0)$.

imation to motion by vector mean curvature. We hope these non-rigorous arguments will encourage the development of rigorous convergence proofs, as they did in the case of diffusion generated motion by mean curvature for surfaces.

We present two alternative approaches: heuristic analysis that uses a variety of shortcuts to deduce the motion law, and a detailed asymptotic analysis that yields the motion law.

3.1 Heuristic Analyses

Here we present a short, formal calculation which "shows" that diffusion generates motion by vector mean curvature for a filament. These calculations allow us to quickly extract the motion law generated by diffusion, without going through the full details of asymptotic analysis. This is particularly useful for exploring novel diffusion-generated algorithms.

3.1.1 Filament Heuristics

In the case of filament motion, we have the curve initially represented by a complex valued function of the form

$$\chi(\vec{x}) = e^{i\theta(\vec{x})}$$

where $\theta(\vec{x})$ is a real angular coordinate on R^3 that increases by $2\pi m$ around any loop about the filament, where m is the nonzero integer winding number of χ. We identify the filament as the place where χ "vanishes", which in general means the locus of points in R^3 that χ winds around. We will deduce the effect that diffusion has on the location of the zero of χ by direct, formal evaluation of the diffusion equation

$$\chi_t = \nabla^2 \chi.$$

In order to provide a clear intuition, we assume that χ winds around the filament uniformly[5] . Specifically, let $\vec{y}$ denote the closest point on a smooth filament to the point $\vec{x}$ and assume $\theta = m\phi(\vec{x} - \vec{y}, t)$ where $\phi(\vec{x} - \vec{y}, t)$ is the polar angle between $\vec{x} - \vec{y}$ and the Frenet normal to the filament at $\vec{y}$. Detailed asymptotics for initializations based on parallel planes (see Figure 1b) are given in Section 3.2.

Laplacian Heuristic We can simplify the analysis slightly by working with the amplitude and phase of χ so we write

$$\chi(\vec{x}, t) = A(\vec{x}, t)e^{i\theta(\vec{x}, t)}$$

where $A = |\chi|$, and plug this form into the diffusion equation. The real part of this equation yields the amplitude evolution equation

$$A_t = \nabla^2 A - |\nabla\theta|^2 A.$$

When viewed in this decomposition, we see there is a reaction term present that instantaneously drives the amplitude A to 0 at the location of the singularity of $|\nabla\theta|$, which in turn occurs at the center of winding of θ, i.e. at

---

[5]Heuristically, this assumption is reasonable since each diffusion step helps to enforce this type of symmetry near the zero set of χ.

the filament location. (Note that the presumed winding of θ implies that $|\nabla\theta|$ blows up at the filament like m/d, where d is the distance to the filament.) Thus, as expected, the amplitude vanishes at the filament. This decomposition shows how this is enforced by the winding number.

All that remains is to write out the Laplacian in suitable geometric coordinates, and show that it has a term corresponding to advection with a velocity that reduces to $\vec{v} = \kappa\hat{n}$ at the filament, where κ is the curvature and $\hat{n}$ is the Frenet normal vector. Suitable coordinates can be defined as follows: let s be the arclength coordinate along the filament. At a given s value along the filament, there is a plane normal to the filament, and the Frenet normal $\hat{n}$ and binormal $\hat{b}$ unit vectors in this plane define associated Cartesian planar coordinates p, q. Thus (s, p, q) define an orthogonal curvilinear coordinate system (at least, near the filament). In this coordinate system, calculation (see [11] for partial details) shows that the the Laplacian is given by

$$\nabla^2 A = H[H[A]] - \frac{\kappa}{1 - \kappa p} A_p + A_{pp} + A_{qq}$$

where $\kappa(s)$ is the curvature of the filament, and H is the differential operator

$$H[f] = \frac{1}{1 - \kappa p}(f_s - \tau f_\phi)$$

where $\tau(s)$ is the torsion along the filament, and ϕ is the polar angle coordinate in the (p, q) plane. Thus the amplitude equation becomes

$$A_t + \frac{\kappa}{1 - \kappa p} A_p = H^2 A + A_{pp} + A_{qq} - |\nabla\theta|^2 A. \tag{2}$$

Consider the short time effects of the terms of this equation: the singular reaction term drives A to 0 at the filament, and the (p, q) diffusion smoothes this profile into a cylindrically symmetric well. Because the resulting A is constant along the filament, and cylindrically symmetric, it has no s or ϕ dependence, and the H terms vanish. Thus, none of these terms actually produce any initial motion of the $A = 0$ location. The remaining terms in the equation, evaluated at the filament where $p = 0$, reduce to

$$A_t + \kappa A_p = 0$$

which convects the values of A in the (p, q) plane, in the p direction, with speed κ. Thus these terms move the zero of A—and hence the filament—by

the vector mean curvature, initially. See the analysis related to Eq. (15) in Section 3.2 for further details on the asymptotic properties of the reaction-diffusion equation (2).

3.2 Asymptotic Analysis of Diffusion Generated Motion

We next present a detailed matched asymptotic analysis of the ALGORITHM CDGM and show that the algorithm indeed captures the motion by curvature along filament normal direction. As a byproduct, we also obtain the local truncation error: $O(1/|\log(\Delta t)|)$. We find both the outer solution away from the filament core and the inner solution taking account of the core structure before finally matching the two asymptotics. The inner solution reveals how the zero amplitude is generated without the Ginzburg-Landau nonlinearity, a conspired effort of linear diffusion and imposed topological winding number. The zero amplitude is what the numerical algorithm captures to follow the evolution of the filament. We also compare the behavior of the filament core in the algorithm with that of the complex Ginzburg-Landau equation (1). During the diffusive step, the filament core size enlarges in time like $O(\sqrt{\Delta t})$, while the Ginzburg-Landau filament core size remains $O(\epsilon)$ for all time.

Let us consider the diffusion effect on a complex scalar function of the form $\chi_0 = \exp\{i\Theta_0\}$, where Θ_0 is the phase function (counting the angle) about a space curve (the filament) Γ_0. Initially, Θ_0 is as described in Section 3.2, see also Fig. 3(b). Let us examine the effect of short time diffusion on χ_0, especially its phase. Suppose the filament is parameterized by z, that is $\Gamma_0 : (\gamma_1(z), \gamma_2(z), z)$, and denote $\vec{x} = (x_1, x_2, x_3)$, $\vec{\xi} = (\xi_1, \xi_2, \xi_3)$. Introducing complex variables:

$$\tilde{x} = x_1 + ix_2, \; \tilde{\gamma} = \gamma_1 + i\gamma_2, \; \tilde{\xi} = \xi_1 + i\xi_2,$$

we write the initial condition as:

$$\chi_0 = \frac{\tilde{x} - \tilde{\gamma}(x_3)}{|\tilde{x} - \tilde{\gamma}(x_3)|},$$

and the solution is:

$$\chi(t, \vec{x}) = (4\pi t)^{-3/2} \int_{R^3} \exp\{-|\vec{\xi} - \vec{x}|^2/4t\} \frac{\tilde{\xi} - \tilde{\gamma}(\xi_3)}{|\tilde{\xi} - \tilde{\gamma}(\xi_3)|} d\vec{\xi}.$$

12

Making the change of variables: $\vec{\xi} = \vec{x} + \tau\vec{\xi}'$, and $\tau = \sqrt{t}$, we have (ignoring the primes):

$$\chi(t, \vec{x}) = (4\pi)^{-3/2} \int_{R^3} \exp\{-|\xi|^2/4\} \frac{\tilde{x} + \tau\tilde{\xi} - \tilde{\gamma}(x_3 + \tau\xi_3)}{|\tilde{x} + \tau\tilde{\xi} - \tilde{\gamma}(x_3 + \tau\xi_3)|} \, d\vec{\xi}. \qquad (3)$$

For any two complex numbers ζ and η, if $\frac{|\eta|}{|\zeta|} \ll 1$, then:

$$
\begin{aligned}
\frac{\zeta + \eta}{|\zeta + \eta|} &= (\frac{\zeta}{|\zeta|} + \frac{\eta}{|\zeta|})((1 + Re(\eta/\zeta))^2 + (Im(\eta/\zeta))^2)^{-1/2} \\
&= (\frac{\zeta}{|\zeta|} + \frac{\eta}{|\zeta|})(1 - Re(\eta/\zeta) + O(|\eta/\zeta|^2)) \\
&= \frac{\zeta}{|\zeta|} + (\frac{\eta}{|\zeta|} - \frac{\zeta}{|\zeta|}Re(\eta/\zeta)) + O(|\eta/\zeta|^2). \qquad (4)
\end{aligned}
$$

Let us now apply (4) with:

$$\zeta = \tilde{x} - \tilde{\gamma}(x_3), \ \eta = \tau\tilde{\xi} + \tilde{\gamma}(x_3) - \tilde{\gamma}(x_3 + \tau\xi_3).$$

Noticing that:

$$\eta = \tau(\tilde{\xi} - \tilde{\gamma}'(x_3)\xi_3) + O(\tau^2\xi_3^2),$$

we have from (3) and (4) the expansion:

$$
\begin{aligned}
\chi(t, \vec{x}) &= \chi(0, \vec{x}) + \tau(4\pi)^{-3/2} \int \exp\{-|\xi|^2/4\} \, L(\xi, x) \, d\xi \\
&+ \tau^2(4\pi)^{-3/2} \int \exp\{-|\xi|^2/4\} \, O(|\xi/\zeta|^2) \, d\xi, \qquad (5)
\end{aligned}
$$

provided $|\eta| \ll |\zeta|$. Here L is linear in ξ. Since $\eta = O(\tau)$, (5) is valid if $|\zeta| = |\tilde{x} - \tilde{\gamma}(x_3)| \gg O(\tau) = O(t^{1/2})$. One can view (5) as a moment expansion with respect to unit Gaussian. The first moment term is equal to zero. So for small t, if $|\tilde{x} - \tilde{\gamma}(x_3)| \geq O(\delta_1) \gg t^{1/2}$, $\delta_1 \in (0, 1)$ a fixed number, we have:

$$\chi(t, \vec{x}) = \chi(0, \vec{x}) + O(t), \qquad (6)$$

or:

$$\bar{\chi} = \chi(t, \vec{x})/|\chi(t, \vec{x})| = \exp\{i\Theta_0 + O(t)\}. \qquad (7)$$

The $O(\tau^2) = O(t)$ term (second moment) in (5) is not zero in general, so (7) is optimal. It says that the effect of small time diffusion on the phase

13

is to introduce an $O(t)$ correction at points away from the filament with a distance much larger than $O(t^{1/2})$. This completes the outer expansion of solution.

Next we look at $\chi(t, \vec{x})$ using Frenet coordinate attached on the filament and develop the inner asymptotic expression for any point within $O(\delta_2)$ distance of filament, $\delta_2 \in (\delta_1, 1)$. Then we match the two expansions at distance between δ_1 and δ_2.

Let us adopt the framework in [4] and define $\Gamma : \vec{X}(s, t) = (X, Y, Z)(s, t)$, where s is the arclength of Γ_0 at $t = 0$. A space vector $\vec{x} = \vec{X} + r\hat{r}$, where $\hat{r} = \hat{r}(\theta, s, t)$, and $\hat{r}$ the radial unit vector on the Frenet plane spanned by $(\hat{n}, \hat{b})$, the normal and binormal unit vectors. Let $\cos(\varphi) = \hat{r} \cdot \hat{n}$, and $\theta_0 = \theta_0(s, t)$ obey: $\theta_{0,s} = -\sigma T$, where $\sigma = |\vec{X}_s|$, and $T = -\sigma^{-1}\hat{b}_s \cdot \hat{n}$, being the torsion of the filament. Let $\theta = \varphi - \theta_0$, then (r, θ, s) form orthogonal curvilinear coordinates, and:

$$d\vec{x} = \hat{r}dr + r\hat{\theta}d\theta + h_3\hat{\tau}ds,$$

where $\hat{\tau}$ the tangential unit vector, $h_3 = \sigma[1 - \kappa r \cos(\theta + \theta_0)]$, and $\kappa = \sigma^{-1}|\hat{\tau}_s|$ the filament curvature.

The heat equation in the (r, θ, s) coordinates is:

$$\left[\frac{\partial}{\partial t} - \dot{\vec{X}} \cdot \nabla_{r,\theta,s} - \frac{r}{h_3}(\hat{r}_t \cdot \hat{\tau})\frac{\partial}{\partial s} - (\hat{r}_t \cdot \hat{\theta})\frac{\partial}{\partial \theta} \right] \chi$$
$$= (rh_3)^{-1}\left[\frac{\partial}{\partial r}(rh_3\frac{\partial}{\partial r}) + \frac{\partial}{\partial \theta}(h_3 r^{-1}\frac{\partial}{\partial \theta}) + \frac{\partial}{\partial s}(rh_3^{-1}\frac{\partial}{\partial s}) \right] \chi \qquad (8)$$

where: $\nabla_{r,\theta,s} = \frac{\partial}{\partial r}\hat{r} + r^{-1}\frac{\partial}{\partial \theta}\hat{\theta} + h_3^{-1}\frac{\partial}{\partial s}\hat{\tau}$. The right hand side of (8) is equal to:

$$[\frac{\partial^2}{\partial r^2} + r^{-1}\frac{\partial}{\partial r} - \frac{\kappa \cos \varphi}{1 - \kappa r \cos \varphi}\frac{\partial}{\partial r} + r^{-2}\frac{\partial^2}{\partial \theta^2}$$
$$+ \frac{\kappa \sin \varphi}{1 - \kappa r \cos \varphi}r^{-1}\frac{\partial}{\partial \theta} + h_3^{-2}\frac{\partial^2}{\partial s^2} - \frac{h_{3,s}}{h_3}\frac{\partial}{\partial s}]\chi.$$

We expand χ as:

$$\chi \sim Ae^{iS} = (A_0 + \delta A_1 + \cdots)(\eta, \tau, s, \theta, t)e^{i(S_0 + \delta S_1 + \cdots)(\eta, \tau, s, \theta, t)}, \qquad (9)$$

14

where $\eta = r/\delta$, $\tau = t/\delta^2$, and $\delta \in (0, \delta_2)$. The heat equation in (η, τ, s, θ) is:

$$[\delta^{-2}\frac{\partial}{\partial\tau} - \dot{X} \cdot \nabla_{\eta\delta,\theta,s} - \delta\eta h_3^{-1}(\hat{r}_t \cdot \hat{\tau})\frac{\partial}{\partial s} - \hat{r}_s \cdot \hat{\theta}\frac{\partial}{\partial\theta}]\chi$$

$$= [\delta^{-2}(\frac{\partial^2}{\partial\eta^2} + \eta^{-1}\frac{\partial}{\partial\eta}) - \delta^{-1}\frac{\kappa\cos\varphi}{1 - \delta\eta\kappa\cos\varphi}\frac{\partial}{\partial\eta}$$

$$+ \delta^{-2}\eta^{-2}\frac{\partial^2}{\partial\theta^2} + \delta^{-1}\frac{\kappa\sin\varphi}{1 - \delta\eta\kappa\cos\varphi}\eta^{-1}\partial_\theta + h_3^{-2}\frac{\partial^2}{\partial s^2} - \frac{h_{3,s}}{h_3}\partial_s]\chi. \quad (10)$$

Plugging (9) into (10) and keeping leading orders $O(\delta^{-2})$ and $O(\delta^{-1})$, we find:

$$\delta^{-2}(A_\tau + iS_\tau A) - \delta^{-1}\dot{X} \cdot \nabla_{\eta,\theta}A = \delta^{-2}[\Delta A + 2i\nabla A \cdot \nabla S - |\nabla S|^2 A +$$
$$iA\Delta S] + \delta^{-1}[-\kappa\hat{n} \cdot \nabla A + iA\kappa\hat{n} \cdot \nabla S]. \quad (11)$$

Collecting imaginary and real parts, we have:

$$S_\tau - \Delta S + 2\frac{\nabla A}{A} \cdot \nabla S + \delta(\kappa\hat{n} - \dot{X}) \cdot \nabla S = O(\delta^2), \quad (12)$$

$$A_\tau - \Delta A + \delta(\kappa\hat{n} - \dot{X}) \cdot \nabla A + |\nabla S|^2 A = O(\delta^2), \quad (13)$$

with initial data for A being 1, and for S the angle variable θ. Here we suppose that the initialization can be expressed as local Frenet coordinates near the filament and that its phase is equal to θ. Otherwise, there is an initial layer during which the phase adjusts itself to θ. Notice that a small interval of t is magnified by δ^{-2} for τ, and so other phase initialization may well have relaxed to θ. The topological constraint on S is that its winding number about the origin is 1, also ∇S tends to zero at ρ infinity which helps to ensure the limit of A equal to one at ρ infinity. In (12)-(13), the coupling term is $\frac{\nabla A}{A} \cdot \nabla S$. To leading order, we have:

$$S_{0,\tau} - \Delta S_0 + 2\frac{\nabla A_0}{A_0} \cdot \nabla S_0 = 0,$$
$$A_{0,\tau} - \Delta A_0 + |\nabla S_0|^2 A_0 = 0, \quad (14)$$

which has solution $A_0 = A_0(|\eta|, \tau) = A_0(\rho, \tau)$, and $S_0 = \theta$. The coupling term is zero, and the reduced A_0 equation becomes:

$$A_{0,\tau} = A_{0,\rho\rho} + \frac{1}{\rho}A_{0,\rho} - \frac{1}{\rho^2}A_0, \quad (15)$$

15

with $A_0(\rho, 0) = 1$. The dynamics of equation (15) is best understood in terms of its self-similar solution:

$$A_0(t, \rho) = A(\frac{\rho^2}{t}) \equiv A(z),$$

satisfying the ODE:

$$A_{zz} + (\frac{1}{z} + \frac{1}{4})A_z - \frac{1}{4z^2}A = 0, \tag{16}$$

with the boundary conditions: $A(z)$ is regular near $z \sim 0$, $A \to 1$ as $z \to +\infty$.

Expanding A for small z, we find two linearly independent local solutions:

$$A_1 = z^{1/2}(c_0 + c_1 z + \cdots), \quad c_0 > 0, \tag{17}$$

and

$$A_2 = z^{-1/2}(b_0 + b_1 z + \cdots) + \log z\, (b_0' + b_1' z + \cdots), \quad b_0 > 0,$$

with the latter removed due to the regularity condition at $z = 0$.

Hence we see from (17) that the desired solution is strictly increasing in a small neighborhood of zero. By the maximum principle on positive solutions of equation (16), such a solution cannot experience an interior maximum, and so must be nondecreasing towards $z \to \infty$. Finite time blowup cannot occur due to boundedness of coefficients for z away from zero.

It remains only to analyze what limit A approaches as $z \to \infty$, a positive finite number or infinity. Making the change of variables:

$$A = e^{-\frac{1}{2}\log z - z/8}B,$$

we have:

$$B_{zz} - q(z)B = B_{zz} - (\frac{1}{64} + \frac{1}{8z})B = 0.$$

By a result of P. Hartman (p. 382, [8]), we have two linearly independent solutions:

$$B \sim q^{-1/4}\exp\{\pm \int^z \sqrt{q(s)}\, ds\}, \quad z \to \infty,$$

where:

$$q^{1/2}(s) = \left(\frac{1}{64} + \frac{1}{8s}\right)^{1/2} \sim \frac{1}{8}\left(1 + \frac{4}{s} - \frac{8}{s^2} + \cdots\right),$$

and:
$$q^{-1/4}(s) = \left(\frac{1}{64} + \frac{1}{8s}\right)^{-1/4} \sim \frac{1}{\sqrt{8}}\left(1 - \frac{2}{s} + \frac{10}{s^2} + \cdots\right).$$

So the two linearly independent solutions are:
$$B_{1,2} \sim \left(1 - \frac{2}{z} + \frac{10}{z^2} + \cdots\right)\exp\{\pm\frac{1}{8}(z + 4\log z + \frac{8}{z} + \cdots)\}.$$

Or in terms of A:
$$A_1 \sim (1 - \frac{2}{z} + \cdots)\exp\{\frac{1}{z} + \cdots\} = (1 - \frac{2}{z} + \cdots)(1 + \frac{1}{z} + \cdots)$$
$$= (1 - 1/z + \cdots) = e^{-1/z}(1 + \alpha_2 z^{-2} + \cdots), \tag{18}$$

and:
$$A_2 \sim e^{-\log z - z/4}(1 - \frac{2}{z} + \cdots)e^{\frac{8}{z}} = \frac{1}{z}e^{-z/4}(1 + \frac{6}{z} + \cdots).$$

Hence up to a multiplicative constant, the asymptotic behavior of A is that $A(z)$ converges to a finite positive constant as $z \to \infty$. We have $A'(z) \geq 0$, and in fact $A'(z) > 0$ for any finite z. Letting $w = A'(z)$, we see that w satisfies the differential inequality:
$$w_{zz} + (1/z + 1/4)w_z - \left(\frac{1}{z^2} + \frac{1}{4z^2}\right)w = -\frac{1}{2z^3}A < 0,$$

implying via maximum principle that the nonnegative function w cannot achieve an interior minimum 0, thus $w > 0$.

We normalize A so that $A(+\infty) = 1$. By maximum principle, such a solution A ($A(0) = 0$, $A'(z) > 0$, $A(+\infty) = 1$) is the unique classical solution. This normalized self-similar solution is selected with initial condition 1 for equation (15).

With the order $O(\delta)$ terms turned on, the system (12)-(13) is coupled, however, the coupling tends to zero as $\rho \to \infty$ since $\nabla A \to 0$ and $A \to 1$. For $\tau \in [0, \tau_0]$, τ_0 a fixed positive number, as $\rho \to \infty$, the S approaches its steady state in τ denoted by S_∞ obeying the equation:
$$-\Delta S_\infty + \delta(\kappa\hat{n} - \dot{X}) \cdot \nabla S_\infty = O(\delta^2), \tag{19}$$

subject to the constraint that its winding number is one and also $\nabla S_\infty = o(1)$ as $\rho \to \infty$. Solution of (19) to $O(\delta)$ is:
$$S_\infty = \eta \int_0^\theta [G_\eta + \delta(\kappa\hat{n} - \dot{X}) \cdot (\cos\theta, \sin\theta)G] \, d\theta, \tag{20}$$